BRIEF REPORT

Regional Heterogeneity of Aortic Histology and Transcriptomes In Young Cynomolgus Monkeys

Naofumi Amioka[1], Sohei Ito[1], Michael K. Franklin[1], Ching-Ling Liang[1],

Yuriko Katsumata[4,5], Lei Cai[1], Ryan E. Temel[1,2,3],

Alan Daugherty[1,2,3], Hong S. Lu[1,2,3], Hisashi Sawada[1,2,3]

1. Saha Cardiovascular Research Center, College of Medicine,
2. Saha Aortic Center, College of Medicine, University of Kentucky, KY
3. Department of Physiology, College of Medicine, University of Kentucky, KY
4. Department of Biostatistics, College of Public Health, University of Kentucky, KY
5. Sanders-Brown Center on Aging, University of Kentucky, KY

Running title: Regional heterogeneity of monkey aortas

Corresponding authors:
Hong S. Lu
Saha Cardiovascular Research Center, University of Kentucky
741 South Limestone Street
BBSRB, B249
Lexington, KY, 40536, USA.
Tel: +1-859-323-4639
E-mail: hong.lu@uky.edu

Hisashi Sawada
Saha Cardiovascular Research Center, University of Kentucky
741 South Limestone Street
BBSRB, B251
Lexington, KY, 40536, USA.
Tel: +1-859-218-1705
E-mail: hisashi.sawada@uky.edu

Word count:
Abstract: 265 words
Manuscript: 4,937 words

ABSTRACT

Background: The regional heterogeneity of vascular components is an important determinant of aortic biology. This notion has been explored in multiple mouse studies, but not in human aortas due to the difficulty of acquiring normal tissues. In the present study, we examined the regional heterogeneity of aortas in healthy non-human primates that have similarities to humans.

Methods: Aortic samples were harvested from the ascending, descending, suprarenal, and infrarenal regions of young cynomolgus monkeys. The regional heterogeneity of aortic structure and transcriptomes were examined by histological and bulk RNA sequencing analyses.

Results: Immunostaining of CD31 and αSMA revealed that endothelial and smooth muscle cells were distributed homogeneously across the aortic regions. In contrast, elastic fibers were less abundant and disorganized in the infrarenal aorta compared to other regions. Bulk RNA sequencing identified differences in collagen mRNA abundance among the regions. *COL1A1,* a major collagen gene, was highly abundant in the infrarenal aorta. Movat's staining revealed consistently that collagen fibers were more abundant in the media and adventitia of the infrarenal aorta than in other regions. Proteoglycan accumulated in the intima of the infrarenal region. Polarized imaging of picrosirius red staining demonstrated that type 1 collagen was distributed predominantly in the adventitia and media of the infrarenal aorta adjacent to disarrayed elastic fibers. Immunostaining of COL1A1 verified type 1 collagen in the intima and adventitia close to the elastic fiber disruption.

Conclusions: Aortas of young cynomolgus monkeys display regional heterogeneity of its transcriptome and the structure of elastin and collagens. Elastic fibers in the infrarenal aorta are disarrayed along with the deposition of collagen fibers and proteoglycan.

NON-STANDARD ABBREVIATIONS

Asc:	ascending thoracic aorta
Dsc:	descending thoracic aorta
Sup:	suprarenal abdominal aorta
Inf:	infrarenal abdominal aorta
EC:	endothelial cell
SMC:	smooth muscle cell
ECM:	extracellular matrix
TGF-β:	transforming growth factor β
COL1A1:	Collagen type 1a1

HIGHLIGHTS

- The present study determined the regional heterogeneity of aortic biology in aortas of young cynomolgus monkeys.
- Aortas of young cynomolgus monkeys displayed region-specific aortic structure and transcriptomes.
- Elastic fibers are disarrayed in the infrarenal aorta along with the deposition of collagen fibers and proteoglycan.

GRAPHIC ABSTRACT

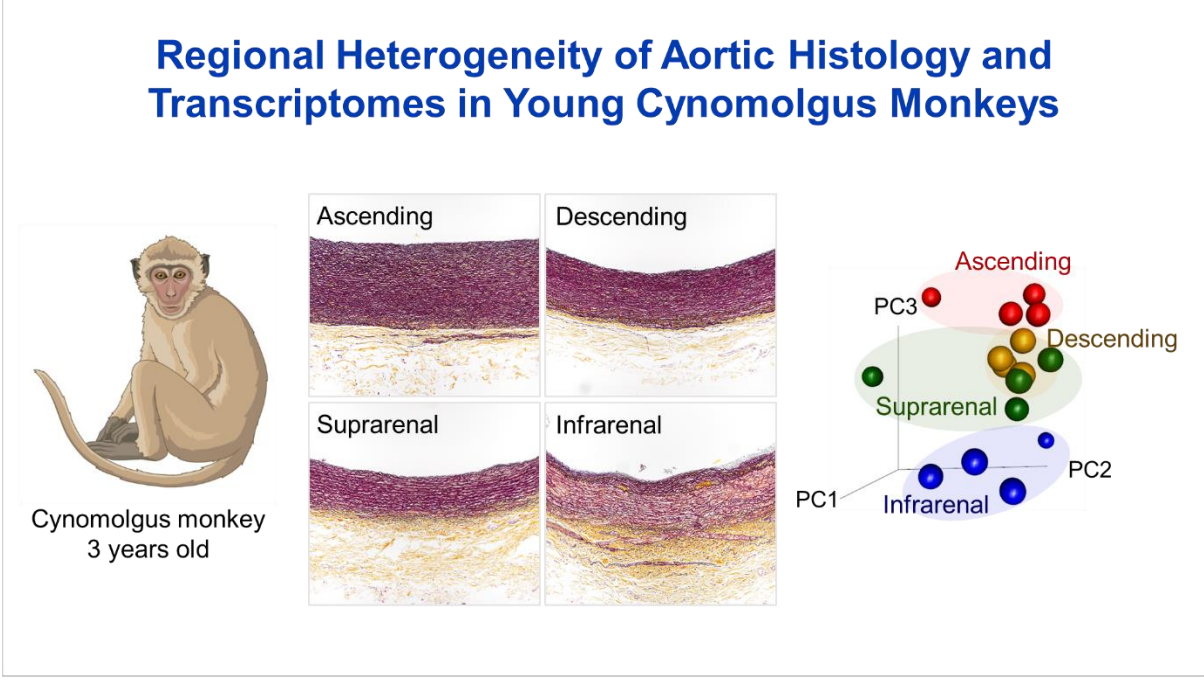

INTRODUCTION

The aorta is the largest vessel in the body that supplies oxygenated blood to the systemic circulation. The aortic wall is composed of three tunicae: intima, media, and adventitia, which primarily contain endothelial cells (ECs), smooth muscle cells (SMCs), and fibroblasts, respectively. These resident cells play pivotal roles in maintaining the integrity of the aortic wall. In addition to these cells, the extracellular matrix (ECM) is also an important structure in the aortic wall. Aortic cells and ECM form a laminar structure cylindrically that confers structural strength and elasticity to the vascular wall.[1, 2] Thus, it is vital to understand the precise roles of these components for advancing our knowledge of aortic biology.

The aorta has four major regions: ascending and descending thoracic regions and suprarenal and infrarenal abdominal regions. Although the laminar structure of the vascular wall is apparently homogeneous throughout the aorta, there is evolving evidence that aortic functions are heterogeneous across the regions. For instance, a previous in vitro study using chick cells demonstrated that SMCs in the aortic arch are more proliferative than those in the infrarenal abdominal aorta.[3] In mice, angiotensin II infusion induces cellular hyperplasia in the ascending aorta but cellular hypertrophy in other regions.[4] Of note, only the infrarenal abdominal region in mice exhibits aortic wall constriction in response to angiotensin II stimuli.[5] These studies support the notion that different aortic regions display distinct biological behaviors. Despite multiple studies in animal models, this hypothesis has not been fully examined in humans. A recent study using aortic images by computational tomography revealed higher vascular stiffness in the infrarenal abdominal aorta than in the ascending aorta.[6] Another study demonstrated the regional variance of collagen and elastin contents histologically using human aortic samples from aged (67-92 years old) subjects.[7] To further understand the regional heterogeneity, it is important to determine histological differences and their molecular basis in young subjects without pathological changes. However, the limited availability of freshly harvested human samples, especially aortas from healthy young individuals, is a significant impediment to the determination of the regional specificity of aortic biology in physiological conditions.

Mice have been used as a common species in preclinical studies to investigate vascular physiology, including the regional heterogeneity of the aorta.[4, 5] However, mice may not mimic the human vascular system. Aortic size and hemodynamics are considerably different between mice and humans.[6] Aortic length is 10 times higher in humans than in mice. Although blood pressure is similar between the species, heart rate is 10 times higher in mice than in humans. Given these differences, studies using mouse models often require validation using human samples for accurate interpretation and translational insights. In contrast, non-human primates have similarities with humans in these aspects. Furthermore, there is a genetic, metabolic, and physiologic closeness between humans and non-human primates.[8] Hence, studies using non-human primates would provide more translational insights into understanding aortic physiology.

In the present study, to understand the histological and transcriptomic heterogeneities across the aortic regions under physiological conditions, histological and bulk RNA sequencing analyses were performed in aortas of young cynomolgus monkeys with generally healthy conditions.

MATERIAL AND METHODS

All numerical data are available in **Supplemental Excel File**. Bulk RNA sequencing data (raw FASTQ and aligned data) will be made publicly available at the gene expression omnibus (GEO) repository.

Monkey

Female Mauritian cynomolgus monkeys were purchased from DSP Research Services (3 years old, n=4). Monkeys were fed Teklad global 20% protein primate diet (#2050, Envigo) and given access to water ad libitum. The room temperature and humidity were maintained at 68 to 74°F and 50 to 60%, respectively. Monkeys were maintained on a 14:10 hour light:dark cycle. After euthanasia by exsanguination under isoflurane anesthesia, aortic tissues were harvested from each region (**Supplemental Figure 1**): the middle ascending aorta (Asc), the middle descending thoracic aorta (Dsc), the suprarenal abdominal aorta proximal to the celiac artery (Sup), and the distal infrarenal abdominal aorta proximal to the bifurcation of iliac arteries (Sup). Aortic samples were either snap-frozen in liquid nitrogen for bulk RNA sequencing or immersed in paraformaldehyde (4% wt/vol, P6148, Sigma-Aldrich) for histological analyses. All protocols were approved by the University of Kentucky IACUC (#2020-3596) in accordance with the National Institutes of Health guidelines.

Histological Staining

Fixed aortas were placed in ethanol (70% vol/vol) for 24 hours, embedded into paraffin, and cut into 5 µm sections. Subsequently, paraffin-embedded sections were deparaffinized using limonene (#183164, Sigma-Aldrich) followed by 2 washes with ethanol (100%) and 1 wash with Automation Buffer (GTX30931, GeneTex).

For immunostaining, deparaffinized sections were incubated with H_2O_2 (1%; H325-500, Fisher Scientific) for 2 minutes at 40°C. Antigen retrieval (HK547-XAK, BioGenex, 20 minutes at 98°C) was applied for CD31 staining. Non-specific binding of primary antibodies was blocked by goat serum (2.5% vol/vol; MP-7451, Vector laboratories) for 20 minutes at room temperature. Sections were next incubated with rabbit alpha-smooth muscle actin (α-SMA) antibody (2 µg/ml, ab5694, abcam) for 30 minutes at room temperature, rabbit CD31 antibody (3 µg/ml, ab28364, abcam) for 12 hours at 4°C, or rabbit COL1A1 antibody (3 µg/ml, ab138492, abcam) for 12 hours at 4°C. Sections were also incubated with a non-immune rabbit IgG antibody (I8140, Sigma-Aldrich) as a negative control. Goat anti-rabbit IgG conjugated with horseradish peroxidase (30 minutes, MP-7451, Vector laboratories) was used as a secondary antibody. ImmPACT® NovaRed (SK4805, Vector) was used as a chromogen. Hematoxylin (26043-05, Electron Microscopy Sciences) was used for counterstaining. Slides were then coverslipped with Permanent Mounting Medium (H-5000, Vector).

Movat's pentachrome staining was performed using a Movat's Pentachrome method for Connective Tissue kit (k042, Poly Scientific R&D) according to the manufacturer's protocol. Verhoeff's iron hematoxylin was performed as described previously.[9, 10] Briefly, deparaffinized sections were incubated with Verhoeff's iron hematoxylin (iodine: 5.3 g/L, potassium iodide: 10.7 g/L, hematoxylin: 2.8% wt/vol, ferric chloride: 2.2% wt/vol) for 20 minutes. Subsequently, the sections were differentiated with 2% ferric chloride for 2 minutes and washed with distilled water. After dehydration,

the sections were cover-slipped with Permount (SP100, Fisher Scientific). For picrosirius red staining, deparaffinized sections were incubated with phosphomolybdic acid (0.2% vol/vol; HT153, Sigma-Aldrich) for 5 minutes followed by staining with picrosirius red and fast green solution: Direct Red 80 (0.1% vol/vol; 365548, Sigma-Aldrich), Fast Green FCF (0.1% wt/vol; F7258, Sigma-Aldrich) in saturated picric acid (1.3% wt/vol; P6744, Sigma-Aldrich), for 60 minutes at room temperature. The slides were then rinsed with acidified water (0.1 N hydrochloride acid, H2505, Aqua Solutions Inc), dehydrated through increasing concentration of ethanol, incubated with three changes of xylene, and coverslipped with DEPEX (50-247-470, Thermo Fisher Scientific).

Histological measurements

Histological images were captured using an Eclipse Ni with DS-Ri2 (Nikon), Optiphot-2 with DS-Ri1 (Nikon), or AxioScan Z7 (Zeiss). The images were analyzed using either NIS-Elements AR software (ver 5.11.03, Nikon) or Zen Blue edition (ver 3.3, Zeiss). Medial thickness was defined as the distance from the inner to external elastic laminae. Internal perimeters were measured by tracing the internal elastic lamina. After the subtraction of the white background, the percent elastin area was measured in the media using the following thresholds: R: 0-255, G: 0-255, B: 27-255. These measurements were performed in four orthogonal locations of each section and means were calculated for statistical analysis. All measurements were verified by a member of the laboratory who was blinded to study groups.

Bulk RNA sequencing

Aortic samples were incubated with RNAlater solution (#AM7020, Invitrogen) for 12 hours. Subsequently, RNA was extracted using RNeasy Fibrous Tissue Mini kits (#74704, Qiagen). mRNA samples were then shipped to Novogene (CA) for bulk mRNA sequencing. cDNA library was generated from total mRNA (1 µg) using NEBNext UltraTM RNA Library Prep Kits for Illumina (New England BioLabs). cDNA libraries were sequenced by NovaSeq 6000 (Illumina) in a paired-end fashion to reach more than 1.5M reads. The Qscore of over 50% bases of the read is ≤5 or reads containing adapter or ploy-N were removed. Paired-end reads were mapped to the cynomolgus reference genome (Macaca_fascicularis_5.0) using HISAT2 (v2.0.5) and quantified using FeatureCounts (v1.5.0-p3).[11, 12]

Statistical Analysis

Statistical analyses were performed using R (v4.2.2).[13] Histological data are presented as a boxplot with the median and 25th/75th percentiles. The histological data were analyzed using a linear mixed effects model with inverse variance weights implemented by “nlme” R package (v3.1-162) followed by Bonferroni correction. Bulk RNA sequencing data were analyzed using a negative binomial mixed effects model with “glmmSeq” R package (v0.5.5).[14] Dispersion parameter estimates and normalization factor calculation using the trimmed mean of M-value (TMM) method were performed by “edgeR” Bioconductor package.[15] Gene ontology enrichment analysis was performed using “clusterProfiler” package (v4.2.2).[16] To consider correlations among four regions within individual mice, random effects were incorporated in both histological

and bulk RNA sequencing data analyses. P<0.05 or Bonferroni/FDR adjusted P<0.05 was considered statistically significant.

RESULTS

Unique structural characteristics of elastic fibers in the infrarenal abdominal aorta

We first performed immunostaining of αSMA and Verhoeff's iron staining to evaluate the regional heterogeneity of the aortic media with a focus on SMCs and elastic fibers (**Figure 1A, B**). The aortic size demonstrated by internal perimeters was largest in the ascending aorta (**Figure 1C**). The aortic media was also most thickened in the ascending aorta (**Figure 1D**), although SMCs were uniformly distributed across the media throughout the aorta (**Figure 1A**). Consistent with the gradient of medial thickness, the ascending aorta had more elastic layers than those of other regions (**Figure 1E**). The number of elastic layers was about 60 and 10 in the ascending and infrarenal abdominal aortas, respectively. Elastic fibers in the ascending, descending, and suprarenal aortas were distributed densely, whereas those in the infrarenal region were thin and their density was less than in other regions (**Figure 1F**). These data showed that the media, especially elastic fibers, displayed region-specific differences in aortas of monkeys.

Homogeneous EC distribution in the aortic intima and vasa vasorum

We next assessed ECs by CD31 immunostaining (**Supplemental Figure 2A, B**). ECs formed a single layer in the intima uniformly in all aortic regions. In addition to the intima, ECs were also observed in vasa vasorum in the adventitia across the regions. Importantly, vasa vasorum were only found in the adventitia, but not in the media. The penetration of vasa vasorum into the media was not observed in any regions. These results indicate the uniformity of EC distribution in the aortic wall.

Collagen-rich transcriptome in the infrarenal abdominal aorta

To explore the regional heterogeneity of aortic transcriptomes, we then performed bulk RNA sequencing using aortic mRNA isolated from each region. Principal component analysis revealed that aortic transcriptomes were different in a region-specific manner (**Figure 2A**). In particular, the infrarenal abdominal aorta exhibited a distinct transcriptome compared to other regions (**Figure 2A, B**). There were 132 differentially expressed genes (DEGs) among 4 regions (**Figure 2B, Supplemental Excel File**). Gene ontology enrichment analysis showed that several annotations related to the regionalization and body axis were significant in these genes (**Figure 2C**). In comparing the infrarenal transcriptome versus other regions, there were 119 (Inf vs Asc), 101 (Inf vs Dsc), and 61 (Inf vs Sup) DEGs (**Supplemental Figure 3A, Supplemental Excel File**). The number of DEGs was decreased along with the regional distance. It is noteworthy that only 10 DEGs were identified in the comparison between the descending thoracic and suprarenal abdominal aortas (**Supplemental Figure 3B**).

Consistent with histological findings that SMCs and ECs were uniformly distributed in the aorta across the regions, the mRNA abundances of EC (*PECAM1*, *VWF*, *CDH5, TEK*) and SMC (*ACTA2*, *MYH11*, *CNN1*, *TAGLN*) marker genes did not

differ among aortic regions (**Figure 2D**). Cell proliferation markers, such as *MKI67*, *MYC*, *KLF4*, and *KLF5*, were also not different among regions (**Supplemental Figure 4A**). Although *ELN* and *FBN1* mRNA abundance were not different among regions **(Supplemental Figure 4B)**, some collagen genes showed region-specific differences (**Figure 2E**). In the ascending aorta, collagen type 4 A3 and 21 A4 (*COL4A3*, *COL21A1*) were more abundant than in the infrarenal aorta, whereas collagen type 1 A1 and 6 A3 (*COL1A1*, *COL6A3*) were more abundant in the infrarenal aorta.

There is compelling evidence that transforming growth factor (TGF-β) signaling and the renin-angiotensin system affect vascular fibrosis.[17-19] Therefore, we assessed molecules related to these pathways (**Supplemental Figure 4C, D**). mRNA abundance of TGF-β ligands (*TGFB1-3*) and receptors (*TGFBR1-2*, *LRP1*) were not different among regions. Major molecules in the renin-angiotensin system, *AGT* (angiotensinogen), *ACE* (angiotensin-converting enzyme), and *AGTR1-2* (angiotensin II type 1 or 2 receptor) were also not different.

Disorganized structure of ECM in the infrarenal abdominal aorta

Transcriptomic analyses revealed region-specific differences of multiple collagen genes. Thus, we next determined the histological distribution of collagen fibers in each aortic region. Movat's pentachrome staining displayed collagen fibers in both the media and adventitia that had a gradient across the aorta that increased from the ascending to infrarenal regions (**Figure 2F**). Consistently, picrosirius red staining also exhibited the trans-aortic gradient of collagen fibers (**Supplemental Figure 5A**). It is of note that, in the media of the infrarenal aorta, collagen deposition predominated in the area having disarrayed elastic fibers (**Figure 2G**). In addition, proteoglycan deposition was observed in the intima adjacent to the collagen deposition and disarrayed elastic fibers in the media (**Figure 2G, Supplemental Figure 5B**). Polarized images revealed that collagen fibers in the media were mixed population of type I and III fibers, while adventitial collagens were type III dominantly (**Figure 2H**). Consistently, immunostaining of COL1A1 demonstrated the deposition of type I collagen in the media contiguous to the intima (**Figure 2I**). These results suggest that the infrarenal aorta of young monkeys, despite being under a healthy condition, exhibits a disorganized ECM structure compared to other regions that is characterized by deposition of collagen and proteoglycan, in addition to elastic fiber disruption.

DISCUSSION

The present study profiled aortic cells and ECM in four aortic regions of young cynomolgus monkeys by histological and transcriptomic approaches. The infrarenal abdominal aorta displayed disarrayed elastic fibers with collagen and proteoglycan deposition. The transcriptomic analysis also identified region-specific divergence in collagen-related genes. This study highlighted the regional heterogeneity of ECM structure in aortas of young non-human primates.

ECM plays a crucial role in maintaining the structural integrity and functions of the aorta. Elastic and collagen fibers are key components of ECM and these fibers collaborate to provide elasticity and strength to the vessel wall.[2, 20, 21] Thus, the disruption of these fibers has been considered to underlie aortic diseases, such as aneurysms and dissections. This premise is enhanced by fragmentation of elastic fibers

and collagen deposition being prominent features of these diseases.[22-24] In the present study, we found fragmented elastic fibers in the media and collagen deposition in the media and adventitia of the infrarenal abdominal aortas, but not other regions. Thus, these results suggest a structural frailty of the infrarenal aorta. It remains to be determined the impact of these structural differences on biomechanical strength of the aortic wall. Importantly, these “pathologies” in the infrarenal aorta were observed in aortas of young monkeys under a healthy condition. It would be interesting to determine how these histological features are changed during disease development and progression.

Human aortic aneurysms occur in a region-specific manner with the infrarenal abdominal aorta being a common location. Several mechanisms have been reported as a determinant of the regional specificity of aortic aneurysms, such as hemodynamic effects, embryonic origins of SMCs, and structural heterogeneity.[9, 25-29] Multiple studies have shown that structural components of the aortic wall vary by region. The thickness of the aortic adventitia is significantly increased from the ascending to the infrarenal regions.[7, 30] In contrast, the medial thickness is decreased from the ascending to the descending aorta. Consistent with these studies, the trans-aortic gradient of medial and adventitial thickness was also observed in the present studies. In addition to the gradient, the present study also identified ECM disruption only in the infrarenal aorta. Given the important role of ECM in the integrity of the aortic wall, the region-specific ECM disruption may contribute to the regional specificity of aortic aneurysms.

Vasa vasorum form a microvascular network that supplies oxygen and nutrients to the vascular wall.[31-33] They are also linked to development of vascular diseases, including aortic aneurysms.[34, 35] Previous studies investigating vasa vasorum formation in multiple species reported that vasa vasorum were observed in the media from the ascending to the suprarenal abdominal aorta, but not in the infrarenal abdominal aorta, in humans.[36-38] Based on the number of elastic fibers in each aortic region, this study concluded that medial vasa vasorum in mammals was not present in the aortic wall having less than 29 elastic layers. It has been thought that the absence of medial vasa vasorum in the infrarenal aorta contributes to the regional heterogeneity of aortic aneurysms.[34, 35] In our study, vasa vasorum was identified in the adventitia throughout the aorta. Meanwhile, medial vasa vasorum was not observed in either aortic region, including the ascending aorta that had more than 29 elastic layers. Therefore, there is an inconsistency regarding the presence of vasa vasorum in the aortic media. However, the present study examined vasa vasorum in young monkeys (3 years old = equivalent to 9 years old in humans) corresponding to the pubescent age in humans,[39] whereas the previous studies used aortas at 20-50 years of age.[38] Therefore, vasa vasorum has the potential of changing its distribution during aging. Further studies are needed to investigate the determinants of the distribution of vasa vasorum in the aorta.

Studies using non-human primates are time- and cost-consuming compared to mouse studies. In addition, experimental approaches to generate some aortic diseases, such as aneurysms and dissections, have not been developed in monkeys. Thus, a technical breakthrough is needed to advance research approaches in studies using non-human primates, especially for aortic aneurysms. However, non-human primates have clinical relevance because of their biological and anatomical similarities to humans. Thus, the present study provides translational insights into further

understanding aortic biology. Considering the limited availability of aortas from healthy humans, our study using aortas from healthy young non-human primates leads to a greater understanding of aortic functions under physiological conditions.

In conclusion, our study demonstrated the regional heterogeneity of ECM structure and collagen-related transcriptomic profiles in aortas from young cynomolgus monkeys. Despite coming from healthy monkeys, the infrarenal abdominal aorta displayed disarrayed elastic fibers along with an increase of collagen fibers and proteoglycan deposition.

Sources of Funding

This project was supported by the National Heart, Lung, and Blood Institute of the National Institutes of Health (R01HL139748 and R35HL155649) and the American Heart Association SFRN in Vascular Disease (18SFRN33900001 and 33960163). The content in this manuscript is solely the responsibility of the authors and does not necessarily represent the official views of the National Institutes of Health.

Disclosures

None

REFERENCES

1. Wagenseil JE, Mecham RP. Vascular extracellular matrix and arterial mechanics. *Physiol Rev*. 2009;89:957-989
2. Cocciolone AJ, Hawes JZ, Staiculescu MC, Johnson EO, Murshed M, Wagenseil JE. Elastin, arterial mechanics, and cardiovascular disease. *Am J Physiol Heart Circ Physiol*. 2018;315:H189-h205
3. Topouzis S, Majesky MW. Smooth muscle lineage diversity in the chick embryo. Two types of aortic smooth muscle cell differ in growth and receptor-mediated transcriptional responses to transforming growth factor-beta. *Dev Biol*. 1996;178:430-445
4. Owens AP, 3rd, Subramanian V, Moorleghen JJ, Guo Z, McNamara CA, Cassis LA, Daugherty A. Angiotensin II induces a region-specific hyperplasia of the ascending aorta through regulation of inhibitor of differentiation 3. *Circ Res*. 2010;106:611-619
5. Rateri DL, Moorleghen JJ, Balakrishnan A, Owens AP, 3rd, Howatt DA, Subramanian V, Poduri A, Charnigo R, Cassis LA, Daugherty A. Endothelial cell-specific deficiency of Ang II type 1a receptors attenuates Ang II-induced ascending aortic aneurysms in LDL receptor-/- mice. *Circ Res*. 2011;108:574-581
6. Hopper SE, Cuomo F, Ferruzzi J, Burris NS, Roccabianca S, Humphrey JD, Figueroa CA. Comparative study of human and murine aortic biomechanics and hemodynamics in vascular aging. *Front Physiol*. 2021;12:746796
7. Concannon J, Dockery P, Black A, Sultan S, Hynes N, McHugh PE, Moerman KM, McGarry JP. Quantification of the regional bioarchitecture in the human aorta. *J Anat*. 2020;236:142-155
8. Cox LA, Olivier M, Spradling-Reeves K, Karere GM, Comuzzie AG, VandeBerg JL. Nonhuman primates and translational research-cardiovascular disease. *ILAR J*. 2017;58:235-250
9. Sawada H, Katsumata Y, Higashi H, Zhang C, Li Y, Morgan S, Lee LH, Singh SA, Chen JZ, Franklin MK, Moorleghen JJ, Howatt DA, Rateri DL, Shen YH, LeMaire SA, Aikawa M, Majesky MW, Lu HS, Daugherty A. Second heart field-derived cells contribute to angiotensin II-mediated ascending aortopathies. *Circulation*. 2022;145:987-1001
10. Chen JZ, Sawada H, Ye D, Katsumata Y, Kukida M, Ohno-Urabe S, Moorleghen JJ, Franklin MK, Howatt DA, Sheppard MB, Mullick AE, Lu HS, Daugherty A. Deletion of AT1a (angiotensin II type 1a) receptor or inhibition of angiotensinogen synthesis attenuates thoracic aortopathies in fibrillin1$^{C1041G/+}$ mice. *Arterioscler Thromb Vasc Biol*. 2021;41:2538-2550
11. Kim D, Paggi JM, Park C, Bennett C, Salzberg SL. Graph-based genome alignment and genotyping with HISAT2 and HISAT-genotype. *Nat Biotechnol*. 2019;37:907-915
12. Liao Y, Smyth GK, Shi W. featureCounts: an efficient general purpose program for assigning sequence reads to genomic features. *Bioinformatics*. 2014;30:923-930
13. Team RC. R: A language and environment for statistical computing. *R Foundation for Statistical Computing*. 2021: https://www.R-project.org/

14. Surace MLKGESCCA. glmmSeq: General Linear Mixed Models for Gene-level Differential Expression. 2011;R package version 0.5.4:https://github.com/myles-lewis/glmmSeq
15. Robinson MD, McCarthy DJ, Smyth GK. edgeR: a Bioconductor package for differential expression analysis of digital gene expression data. *Bioinformatics*. 2010;26:139-140
16. Wu T, Hu E, Xu S, Chen M, Guo P, Dai Z, Feng T, Zhou L, Tang W, Zhan L, Fu X, Liu S, Bo X, Yu G. clusterProfiler 4.0: A universal enrichment tool for interpreting omics data. *Innovation (Camb)*. 2021;2:100141
17. Ruiz-Ortega M, Rodríguez-Vita J, Sanchez-Lopez E, Carvajal G, Egido J. TGF-beta signaling in vascular fibrosis. *Cardiovasc Res*. 2007;74:196-206
18. Ruiz-Ortega M, Ruperez M, Esteban V, Egido J. Molecular mechanisms of angiotensin II-induced vascular injury. *Curr Hypertens Rep*. 2003;5:73-79
19. Wang W, Huang XR, Canlas E, Oka K, Truong LD, Deng C, Bhowmick NA, Ju W, Bottinger EP, Lan HY. Essential role of Smad3 in angiotensin II-induced vascular fibrosis. *Circ Res*. 2006;98:1032-1039
20. Tsamis A, Krawiec JT, Vorp DA. Elastin and collagen fibre microstructure of the human aorta in ageing and disease: a review. *J R Soc Interface*. 2013;10:20121004
21. Vouyouka AG, Pfeiffer BJ, Liem TK, Taylor TA, Mudaliar J, Phillips CL. The role of type I collagen in aortic wall strength with a homotrimeric. *J Vasc Surg*. 2001;33:1263-1270
22. Campa JS, Greenhalgh RM, Powell JT. Elastin degradation in abdominal aortic aneurysms. *Atherosclerosis*. 1987;65:13-21
23. Nakashima Y. Pathogenesis of aortic dissection: elastic fiber abnormalities and aortic medial weakness. *Ann Vasc Dis*. 2010;3:28-36
24. Wang X, LeMaire SA, Chen L, Shen YH, Gan Y, Bartsch H, Carter SA, Utama B, Ou H, Coselli JS, Wang XL. Increased collagen deposition and elevated expression of connective tissue growth factor in human thoracic aortic dissection. *Circulation*. 2006;114:I200-205
25. den Reijer PM, Sallee D, 3rd, van der Velden P, Zaaijer ER, Parks WJ, Ramamurthy S, Robbie TQ, Donati G, Lamphier C, Beekman RP, Brummer ME. Hemodynamic predictors of aortic dilatation in bicuspid aortic valve by velocity-encoded cardiovascular magnetic resonance. *J Cardiovasc Magn Reson*. 2010;12:4
26. Jana S, Hu M, Shen M, Kassiri Z. Extracellular matrix, regional heterogeneity of the aorta, and aortic aneurysm. *Exp Mol Med*. 2019;51:1-15
27. Sawada H, Rateri DL, Moorleghen JJ, Majesky MW, Daugherty A. Smooth muscle cells derived from second heart field and cardiac neural crest reside in spatially distinct domains in the media of the ascending aorta-Brief report. *Arterioscler Thromb Vasc Biol*. 2017;37:1722-1726
28. Sawada H, Chen JZ, Wright BC, Sheppard MB, Lu HS, Daugherty A. Heterogeneity of aortic smooth muscle cells: A determinant for regional characteristics of thoracic aortic aneurysms? *J Transl Int Med*. 2018;6:93-96
29. Majesky MW. Developmental basis of vascular smooth muscle diversity. *Arterioscler Thromb Vasc Biol*. 2007;27:1248-1258

30. Sokolis DP. Passive mechanical properties and structure of the aorta: segmental analysis. *Acta Physiol (Oxf)*. 2007;190:277-289
31. Heistad DD, Marcus ML, Larsen GE, Armstrong ML. Role of vasa vasorum in nourishment of the aortic wall. *Am J Physiol*. 1981;240:H781-787
32. Mulligan-Kehoe MJ. The vasa vasorum in diseased and nondiseased arteries. *Am J Physiol Heart Circ Physiol*. 2010;298:H295-305
33. Mulligan-Kehoe MJ, Simons M. Vasa vasorum in normal and diseased arteries. *Circulation*. 2014;129:2557-2566
34. Tanaka H, Zaima N, Sasaki T, Hayasaka T, Goto-Inoue N, Onoue K, Ikegami K, Morita Y, Yamamoto N, Mano Y, Sano M, Saito T, Sato K, Konno H, Setou M, Unno N. Adventitial vasa vasorum arteriosclerosis in abdominal aortic aneurysm. *PLoS One*. 2013;8:e57398
35. Tanaka H, Zaima N, Sasaki T, Sano M, Yamamoto N, Saito T, Inuzuka K, Hayasaka T, Goto-Inoue N, Sugiura Y, Sato K, Kugo H, Moriyama T, Konno H, Setou M, Unno N. Hypoperfusion of the Adventitial Vasa Vasorum Develops an Abdominal Aortic Aneurysm. *PLoS One*. 2015;10:e0134386
36. Wolinsky H, Glagov S. Nature of species differences in the medial distribution of aortic vasa vasorum in mammals. *Circ Res*. 1967;20:409-421
37. Wolinsky H, Glagov S. Comparison of abdominal and thoracic aortic medial structure in mammals. Deviation of man from the usual pattern. *Circ Res*. 1969;25:677-686
38. Wolinsky H. Comparison of medial growth of human thoracic and abdominal aortas. *Circ Res*. 1970;27:531-538
39. Kiland JA, Gabelt BT, Kaufman PL. Relationship of aqueous outflow resistance to age and total volume perfused in rhesus and cynomolgus monkeys. *Invest Ophthalmol Vis Sci*. 2011;52:6820-6824

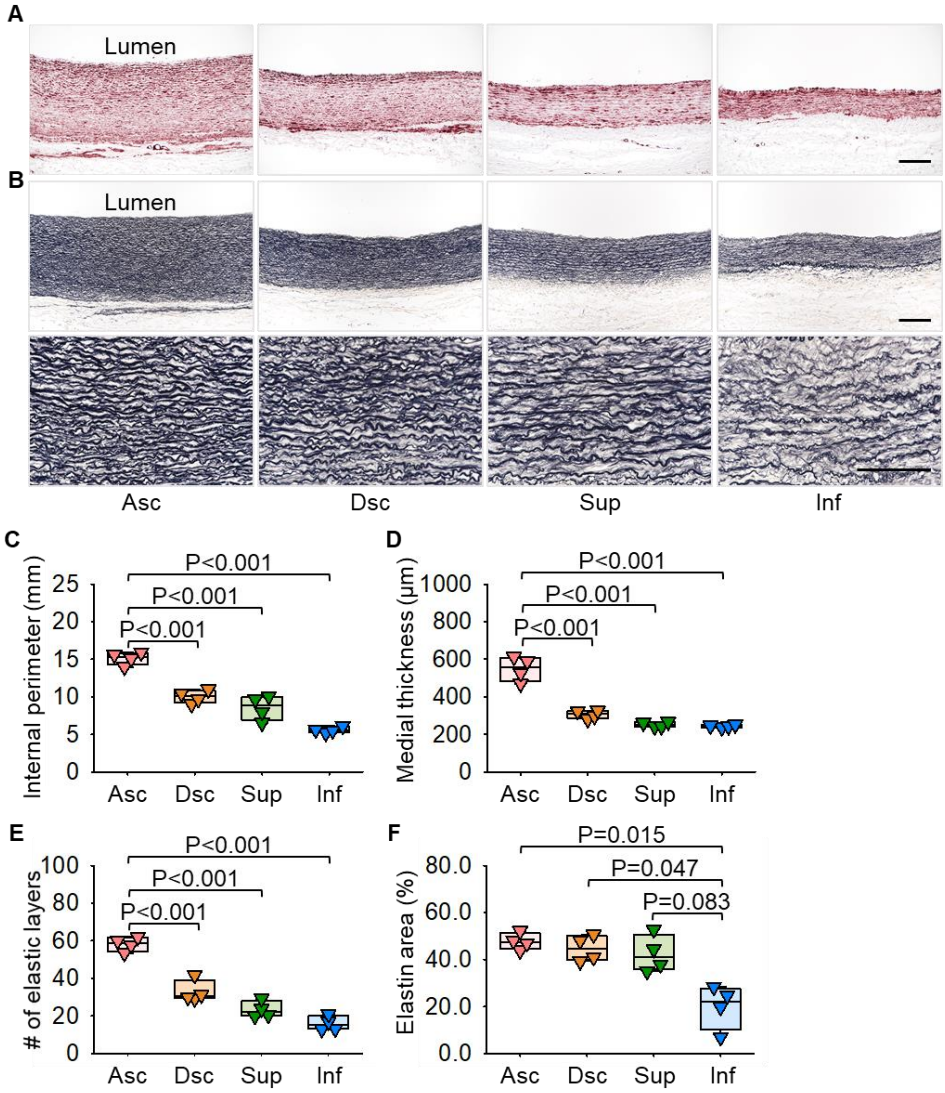

Figure 1. Structural differences of aortic media in young cynomolgus monkeys. Representative images of **(A)** immunostaining for α smooth muscle actin (αSMA) and **(B)** Verhoeff's iron hematoxylin staining. Quantification of **(C)** internal perimeter**, (D)** medial thickness, **(E)** the number of elastic layers, and **(F)** percent elastic area in each region. n=4 per aortic region. Asc indicates ascending; Dsc, descending; Sup, supra-renal; Inf, infra-renal aorta. Scale bars = 200 µm. P values were calculated using a linear mixed effects model with inverse variance weights was used to consider correlation within individual monkeys followed by Bonferroni correction.

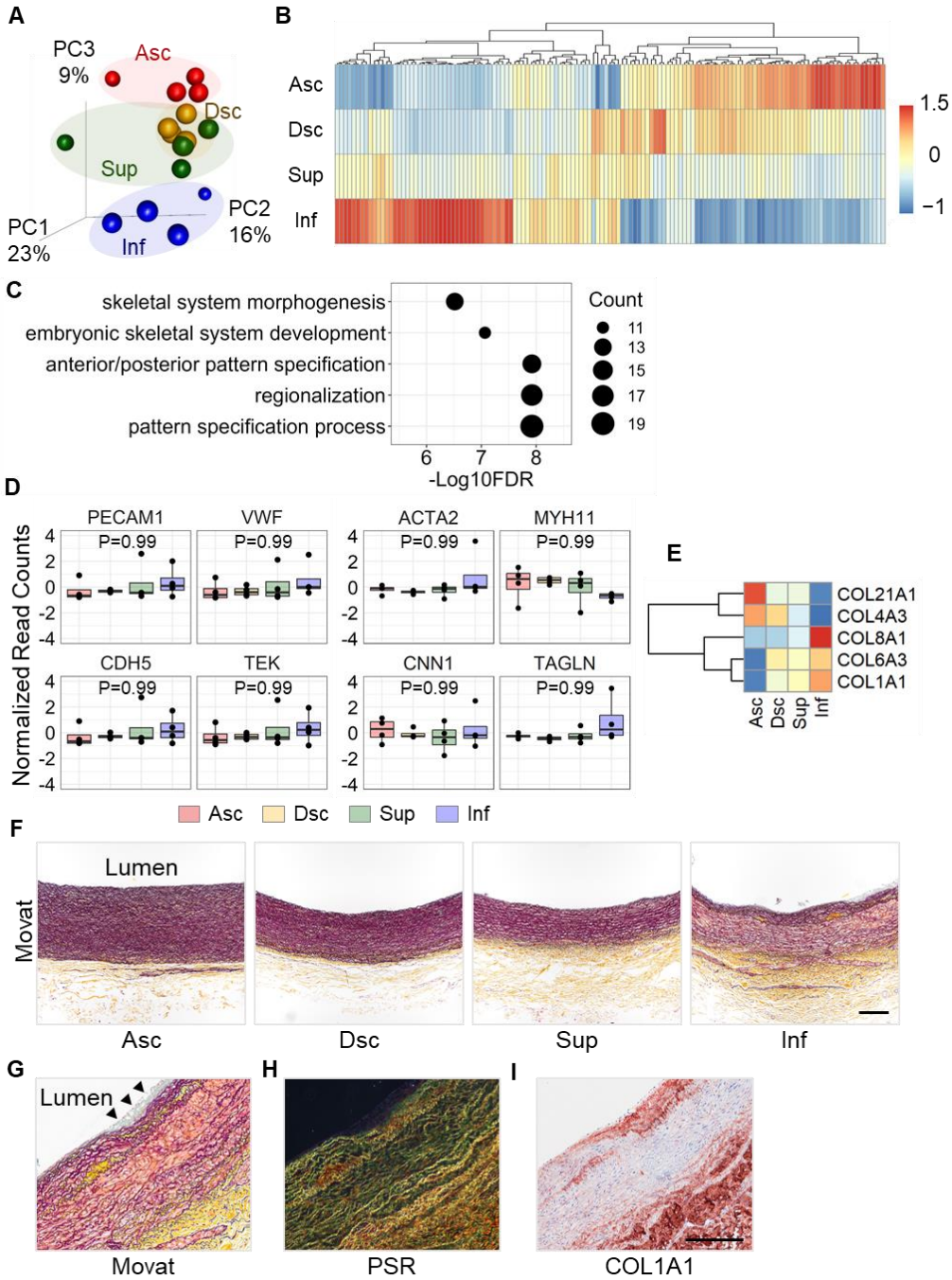

Figure 2. Region-specific transcriptomes and disruption of the extracellular matrix in the infrarenal aorta of cynomolgus monkeys. (A) Principal component analysis for unfiltered transcriptomes. **(B)** Heatmap with Z scored coloring and **(C)** gene ontology enrichment analysis for overall differentially expressed genes (DEGs) identified based on the analysis of deviance. **(D)** Box plots for marker genes for endothelial cells (*PECAM1*, *VWF*, *CDH5*, *TEK*) and smooth muscle cells (*ACTA2*, *MYH11*, *CNN1*, *TAGLN*). **(E)** Z-scored heatmap for collagen-related DEGs. n=4 per aortic region. Representative images of **(F)** Movat's pentachrome staining. High-magnification images of **(G)** Movat's pentachrome, **(H)** polarized picrosirius red (PSR), and **(I)** collagen type I alpha 1 chain (COL1A1) immunostaining in the infrarenal abdominal aorta. n=4 per aortic region. Asc indicates ascending; Dsc, descending; Sup, supra-renal; Inf, infra-renal aorta. Scale bars = 200 μm. Black triangles indicate proteoglycan deposition in the intima.